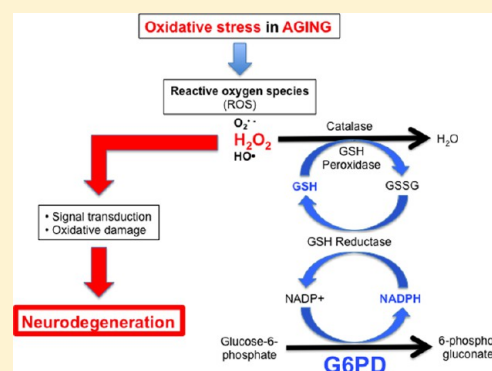


# Brain Glucose-6-phosphate Dehydrogenase Protects against Endogenous Oxidative DNA Damage and Neurodegeneration in Aged Mice

Winnie Jeng<sup>†,§</sup>, Margaret M. Loniewska<sup>†</sup>, and Peter G. Wells<sup>\*,†,‡</sup><sup>†</sup>Faculty of Pharmacy and <sup>‡</sup>Department of Pharmacology and Toxicology, University of Toronto, Toronto, Ontario, Canada

**ABSTRACT:** Glucose-6-phosphate dehydrogenase (G6PD) protects the embryo from endogenous and xenobiotic-enhanced oxidative DNA damage and embryopathies. Here we show in aged mice that G6PD similarly protects against endogenous reactive oxygen species (ROS)-mediated neurodegeneration. In G6PD-normal (G6PD<sup>+/+</sup>) and heterozygous (G6PD<sup>+/def</sup>) and homozygous (G6PD<sup>def/def</sup>) G6PD-deficient male and female mice at about 2 years of age, oxidative DNA damage in various brain regions was assessed by 8-oxo-2'-deoxyguanosine formation using high-performance liquid chromatography and immunohistochemistry. Morphological changes in brain sections were assessed by H&E staining. DNA oxidation was increased in G6PD<sup>def/def</sup> mice in the cortex ( $p < 0.02$ ), hippocampus ( $p < 0.01$ ) and cerebellum ( $p < 0.006$ ) compared to G6PD<sup>+/+</sup> mice, and was localized to distinct cell types. Histologically, in G6PD<sup>+/def</sup> mice, enhanced regionally and cellularly specific neurodegenerative changes were observed in those brain regions exhibiting elevated DNA oxidation, with a 53% reduction in the Purkinje cell count. These results show G6PD is important in protecting against the neurodegenerative effects of endogenous ROS in aging, and suggest that common hereditary G6PD deficiencies may constitute a risk factor for some neurodegenerative diseases.

**KEYWORDS:** Glucose-6-phosphate dehydrogenase, oxidative stress, oxidative DNA damage, neurodegeneration



Glucose-6-phosphate dehydrogenase (G6PD) is a cytoplasmic enzyme responsible for catalyzing the first and rate-limiting step in the hexose monophosphate pathway. The end product of this pathway, ribose-5-phosphate, is required for nucleic acid synthesis and, hence, essential for cell growth. During the conversion of glucose-6-phosphate to 6-phosphogluconolactone, G6PD generates nicotinamide adenine dinucleotide phosphate (NADPH) which, in addition to being essential for many reductive biosynthetic pathways including cholesterol and fatty acid synthesis, also is required for catalase stability and the regeneration of reduced glutathione (GSH).<sup>1</sup> Since catalase and GSH peroxidase are essential for the detoxification of H<sub>2</sub>O<sub>2</sub>, G6PD provides critical protection against reactive oxygen species (ROS) and oxidative stress (Figure 1).

Commonly recognized clinical manifestations of G6PD deficiency include neonatal jaundice, acute hemolytic anemia and life-threatening neonatal kernicterus.<sup>1,2</sup> The inheritance of G6PD shows a characteristic X-linked pattern, with deficiency more likely to affect males than females. G6PD deficiency is the most common human enzymopathy, affecting over 400 million people worldwide with a global prevalence of 4.9%.<sup>3</sup> Over 400 variant G6PD alleles exist in the human population, and to date 186 mutants have been reported.<sup>1,4</sup>

Previously, using a mutant G6PD-deficient mouse model, G6PD was discovered to be a developmentally critical antioxidant enzyme that protects the embryo from the

pathological effects of both endogenous and xenobiotic-enhanced oxidative stress and DNA damage,<sup>5</sup> raising the possibility that G6PD might be similarly important at other times of biochemical susceptibility, such as in aging.

G6PD is constitutively but not uniformly expressed in all cells, with basal activity varying up to about 10-fold among different organs and tissues,<sup>6,7</sup> including in the mutant mouse strain used in the study herein.<sup>5</sup> G6PD activities in the fetus, and in all tissues including brain of young adults of the strain used here, are about 30% and 80% lower in G6PD<sup>+/def</sup> and G6PD<sup>def/def</sup> mice respectively.<sup>5</sup> In various animal models and humans, the levels of mRNA and protein expression in the brain are constitutive in neurons and glial cells.<sup>8–10</sup> With increased oxidative stress, G6PD expression and/or activity *in vitro*<sup>11,12</sup> and *in vivo* is increased.<sup>13,14</sup> Increased neuronal G6PD expression has been observed in the hippocampus of Alzheimer's disease patients compared to age-matched controls.<sup>14</sup>

In this study, we used mutant G6PD-deficient mice to investigate the role of G6PD in protecting against endogenous ROS-mediated oxidative DNA damage and neurodegeneration in the brains of aged mice. This relatively G6PD-deficient strain was used because the knockout is embryolethal.<sup>15</sup> The

**Received:** March 27, 2013

**Accepted:** April 29, 2013

**Published:** April 29, 2013



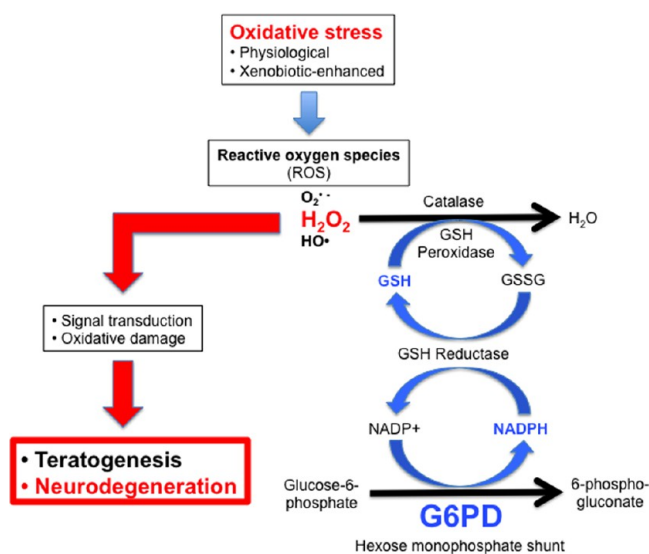


**Figure 1.** Postulated mechanism of neuroprotection against endogenous reactive oxygen species-mediated oxidative stress and damage by glucose-6-phosphate dehydrogenase. The formation of reactive oxygen species (ROS), including superoxide ( $O_2^{\bullet-}$ ), hydrogen peroxide ( $H_2O_2$ ) and hydroxyl radicals ( $HO^{\bullet}$ ), occurs via numerous physiological processes and is enhanced by some xenobiotics. Glucose-6-phosphate dehydrogenase (G6PD), a cytoplasmic enzyme, catalyzes the first step in the hexose monophosphate shunt, also known as the pentose phosphate pathway. The end product of this pathway, ribose-5-phosphate, is required for nucleic acid synthesis, and hence is essential for cell growth. During the conversion of glucose-6-phosphate to 6-phosphogluconate, G6PD generates reduced nicotinamide adenine dinucleotide phosphate (NADPH), essential for catalase stability, many reductive biosynthetic pathways including cholesterol and fatty acid synthesis, and the regeneration of glutathione (GSH) from its oxidized form, glutathione disulfide (GSSG). Catalase and GSH (via GSH peroxidase) are essential for the elimination of  $H_2O_2$ , which, if not detoxified, can alter signal transduction pathways and/or, directly or indirectly via  $HO^{\bullet}$  formation, oxidatively damages cellular macromolecules (DNA, protein, lipid), thereby adversely affecting cellular function. G6PD protects the developing embryo from the pathological effects of endogenous oxidative stress, as well as from xenobiotic-enhanced ROS formation and teratogenesis,<sup>5</sup> and may similarly protect the brain from the neurodegenerative consequences of endogenous ROS-mediated macromolecular damage that accumulates during aging.

deficiency in this strain results from a decrease in total G6PD protein expression causing an overall reduction in activity.<sup>16</sup> The results suggest that G6PD may be an essential protective enzyme preventing ROS-initiated neurodegenerative oxidative damage associated with aging. Since G6PD deficiencies are the most common human enzymopathy,<sup>1</sup> the mutant G6PD-deficient mouse may provide important insights into previously unappreciated risk factors for some neurodegenerative diseases.

## RESULTS

**Increased Oxidatively Damaged DNA in the Brains of Aged G6PD-Deficient Mice.** HPLC-EC was used to quantify the level of endogenous 8-oxo-2'-deoxyguanosine (8-oxo-dG), one form of oxidative DNA damage, in the cortex, hippocampus, striatum, mesencephalon/diencephalon, brainstem and cerebellum of aged G6PD<sup>+/+</sup> and G6PD<sup>def/def</sup> female mice. Aged G6PD<sup>def/def</sup> mice had regionally dependent increases in endogenous brain DNA oxidation compared to their wild-type counterparts (Figure 2). The G6PD<sup>def/def</sup> mice showed a 23%

increase in oxidative DNA damage in the cortex ( $p < 0.02$ ), a 45% increase in the hippocampus ( $p < 0.01$ ), and a 26% increase in the cerebellum ( $p < 0.006$ ) compared to their age-matched G6PD<sup>+/+</sup> mice. No significant differences were observed in the striatum, mesencephalon/diencephalon and brainstem of the deficient mice compared to G6PD-normal controls.

Immunohistochemical staining confirmed the HPLC analysis of increased 8-oxo-dG formation in cortex, hippocampus and cerebellum in the G6PD<sup>+/def</sup> mice compared to the G6PD<sup>+/+</sup> mice (Figure 3). Moreover, oxidative DNA damage was localized to specific regions and cell types. In the cerebellum, the Purkinje cells of G6PD<sup>+/def</sup> mice had increased oxidized DNA (Figure 3B), evidenced by the increased number and intensity of staining, compared to the G6PD<sup>+/+</sup> mice (Figure 3A). Increased localized DNA damage in G6PD<sup>+/def</sup> mice was similarly observed in the cortex and corpus callosum (Figure 3C,D) and the dentate gyrus of the hippocampus (Figure 3E,F), but not in the brainstem (Figure 3G,H).

**Increased Oxidative DNA Damage in Aged G6PD-Deficient Mice Is Associated with Increased CNS Cell Death and Morphological Changes.** The localization of enhanced endogenous ROS-mediated oxidative DNA damage in particular brain regions and cell types of aged G6PD-deficient mice was associated with a similar regional and cellular specificity in enhanced morphological changes in the brains of aged G6PD<sup>+/def</sup> mice assessed semiquantitatively by H&E staining (Figure 4). Some changes characteristic of aging were common to all animals, including reduced Nissl substance and increased neuronal nuclear diameter in the brainstem nuclei (Figure 4Q), scattered apoptotic or pyknotic neuronal bodies in the frontal cortex and hippocampus (Figure 4G), scattered vacuolation in the white matter tracts of the neuropil (Figure 4N), and the accumulation of cytoplasmic lipofuscin (Figure 4R). However, G6PD<sup>+/def</sup> mice exhibited further degenerative changes compared to the age-matched G6PD<sup>+/+</sup> controls. In the cerebellum of the deficient mice, there was increased pathological loss of Purkinje cells at the junction of the molecular and granule cell layers (Figure 4B,D,E) compared to G6PD<sup>+/+</sup> mice (Figure 4A,C). The remaining neurons of the Purkinje layer are characterized by moderate anisokaryosis with a variety of bizarre nuclear shapes (Figure 4E). G6PD-deficient mice also had more vacuolation in the deep cerebellar white matter (Figure 4F).

In the aged G6PD<sup>+/+</sup> mice, there were scattered examples of apoptotic or necrotic bodies, presumably dead or dying neurons, particularly in the outer layers of the parietal cortex. In many cases, the apoptotic remnants have an adjacent astrocyte (Figure 4G). However, in the frontal cortex of the G6PD<sup>+/def</sup> mice, significant changes included an increase in the glia-to-neuron ratio, particularly in the mid to outer regions, and an increased number of chromatolytic or pyknotic neurons in the G6PD<sup>+/def</sup> mice compared to G6PD<sup>+/+</sup> controls (Figure 4H).

The densely packed spherical or oval neurons of the pyramidal layer were normal in the G6PD<sup>+/+</sup> mice with very occasional shrunken neurons in the Ammon's horn. In the polymorph layer, there was patchy condensation of neurons with cell shrinkage and pyknosis. In addition, there were numerous condensed and pyknotic centrally chromatolytic neurons at the lateral border of the hippocampus, as well as in the pyramidal layer (Figure 4J). However, in the G6PD<sup>+/def</sup> mice, there were increased numbers of chromatolytic neurons

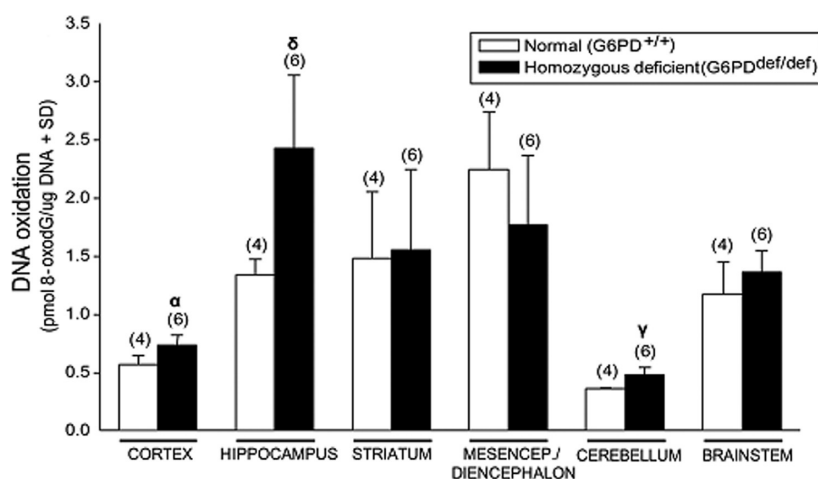


**Figure 2.** Increased levels of DNA oxidation in aged G6PD-deficient mice. Brain regions from G6PD<sup>+/+</sup> and G6PD<sup>def/def</sup> mice were isolated and analyzed by high-performance liquid chromatography with electrochemical detection (HPLC-EC) for oxidatively damaged DNA, quantified by the formation of 8-oxo-2'-deoxyguanosine (8-oxo-dG). <sup>α</sup>*p* < 0.02, <sup>δ</sup>*p* < 0.01 and <sup>γ</sup>*p* < 0.006 compared to aged-matched G6PD<sup>+/+</sup> controls. The number of mice in each group is given in parentheses.

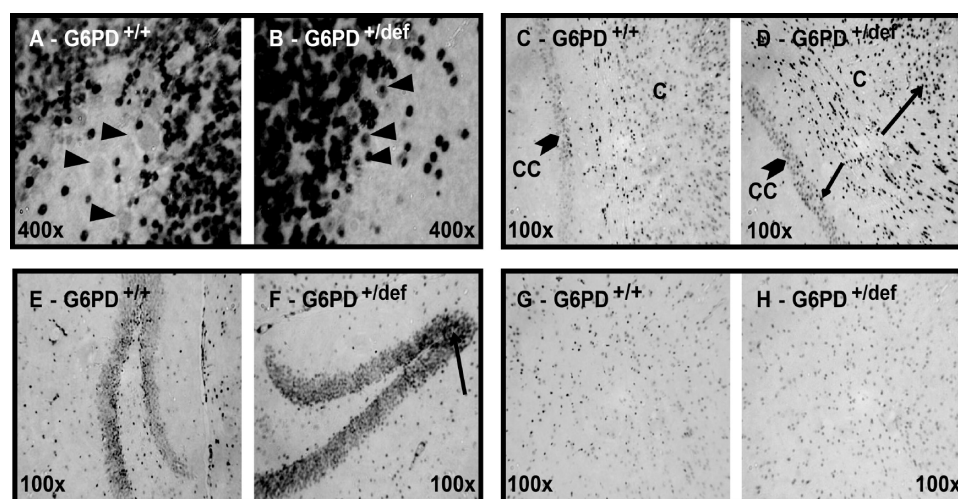


**Figure 3.** Increased localized oxidatively damaged DNA in aged G6PD-deficient mice. G6PD<sup>+/+</sup> and G6PD<sup>+/def</sup> mice were sacrificed and perfused with 10% formalin. Brain sections were analyzed for oxidatively damaged DNA by immunohistochemistry using the N45.1 anti-8-oxo-dG antibody. Immunohistochemical staining is representative of a minimum of *n* = 5/genotype. Comparisons of specific brain areas between paired G6PD<sup>+/+</sup> and G6PD<sup>+/def</sup> mice are enclosed within a black border. (A, C, E, G) G6PD<sup>+/+</sup> mice. (B, D, F, H) G6PD<sup>+/def</sup> mice. (A) Cerebellum from G6PD<sup>+/+</sup> mice: black arrowheads indicate Purkinje cells. (B) Cerebellum from G6PD<sup>+/def</sup> mice: black arrowheads indicate atrophic Purkinje cells with increased oxidatively damaged DNA. (C, D) Cortex (C), corpus callosum (CC); black arrows indicate examples of oxidatively damaged DNA. (E, F) Dentate gyrus of the hippocampus; black arrow indicates increased immunoreactivity to oxidatively damaged DNA. (G, H) brainstem.

within deeper layers of the pyramidal layer (Figure 4K). The pyramidal layer and granule cell layer of the Ammon's horn of the hippocampus and the dentate gyrus, respectively, are characterized by greater vacuolation and spongiosis in the G6PD-deficient mice (Figure 4M) compared to the G6PD<sup>+/+</sup> controls (Figure 4L). In addition, numerous condensed and pyknotic centrally chromatolytic neurons at the lateral border of the hippocampus were observed (Figure 4K), along with scattered examples of large vacuolated mononuclear cells adjacent to blood vessels.

The pathological findings in the brainstem were increased in the aged G6PD<sup>+/def</sup> mice compared to the G6PD<sup>+/+</sup> controls. Although there was increased neuronal nuclear diameter in the brainstem nuclei in the G6PD<sup>+/+</sup> mice, in the G6PD<sup>+/def</sup> mice, the brainstem nuclei had moderate to marked regional accumulation of lipofuscin in neuronal cell bodies, particularly

in the hypoglossal nuclei (Figure 4P). There is also more prominent vacuolation of the white matter tracts in the G6PD<sup>+/def</sup> mice (Figure 4O) than the G6PD<sup>+/+</sup> mice (Figure 4N). Thickening and neoplastic proliferation of cells in the brainstem was seen in one G6PD<sup>+/def</sup> case with mitotic figures scattered throughout the pleomorphic cell population (Figure 4S). The proliferative tissue was characterized by myxomatous tissue composed of stromal fibroblastic cells with a variable degree of differentiation. There were also examples of marked dysplasia/anaplasia in the cell population with up to 3× anisokaryosis. The G6PD<sup>+/def</sup> mice also showed more examples of foamy and vacuolated mononuclear cells compared to G6PD<sup>+/+</sup> mice (Figure 4I).

Increased lipofuscin accumulation was seen in the frontal cortex, hippocampus and cerebellum in the G6PD<sup>+/def</sup> mice.



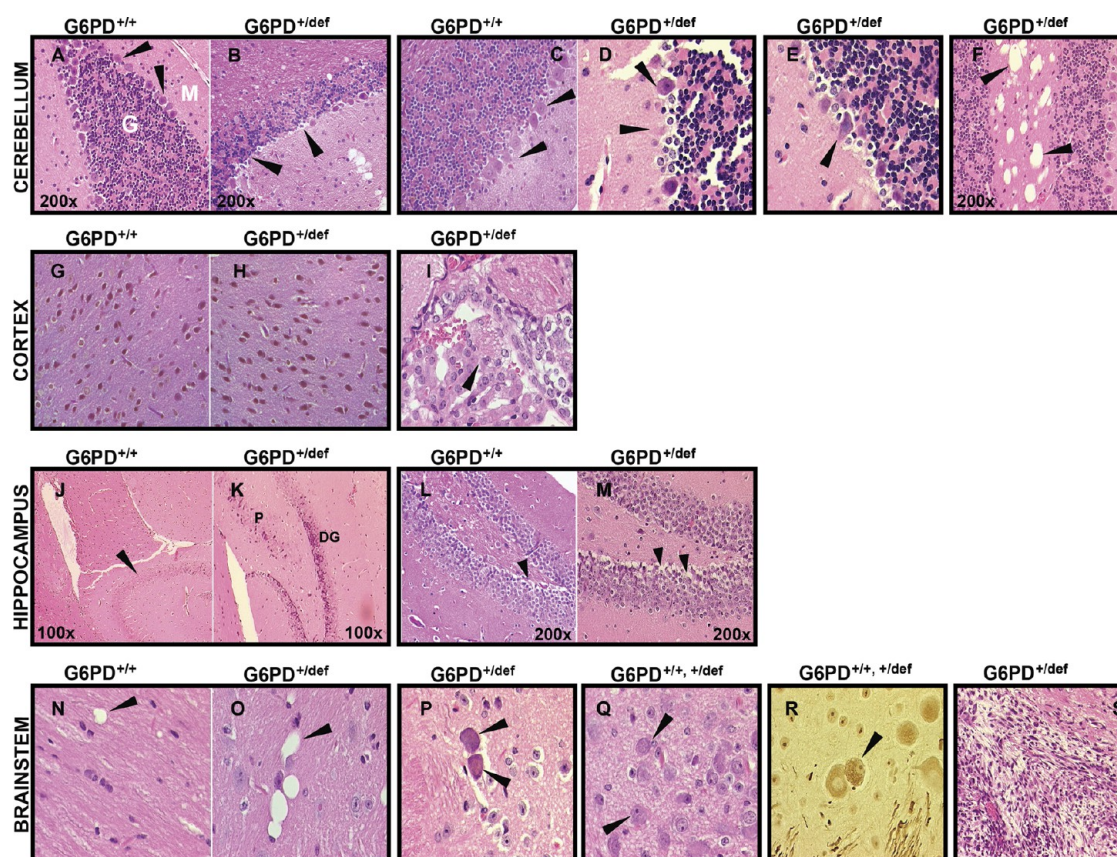


**Figure 4.** Increased CNS cell death and morphological changes in aged G6PD-deficient mice. Brain sections from G6PD<sup>+/+</sup> and G6PD<sup>+/-</sup> mice were stained with H&E and analyzed for morphological changes, with panels representative of a minimum of  $n = 5$ /genotype. The brain area is shown by row. Comparisons of specific brain areas between paired G6PD<sup>+/+</sup> and G6PD<sup>+/-</sup> mice are enclosed within a black border. (A, C, G, J, L, N) G6PD<sup>+/+</sup> mice. (B, D, E, F, H, I, K, M, O, P, S) G6PD<sup>+/-</sup> mice. (Q, R) Common to both G6PD<sup>+/+</sup> and G6PD<sup>+/-</sup> mice. (A, C) Purkinje cells (black arrow heads), and granular (G) and molecular (M) layers of the cerebellum. (B, D) Loss of Purkinje cells. (E) Moderate anisokaryosis and bizarre nuclear Purkinje cells. (F) Vacuolation in the deep cerebellar white matter. (G) Chromatolytic or pyknotic neurons in the frontal cortex, which are increased in H, where they are often associated with astrocytes. (I) Single, foamy and vacuolated mononuclear cell in lumen of dorsal third ventricle. (J) lateral boundary of hippocampal formation (black arrowhead). (K) Condensed neurons in both pyramidal layer (P) of hippocampus and granular layer of dentate gyrus (DG). (L) Vacuolation and spongiosis (black arrowhead) of hippocampus, which is increased in M. (N) White matter vacuolation of brainstem, which is increased in O. (P) Lipofuscin in neuronal cell bodies of the brainstem. (Q, R) Pathological changes common to both G6PD<sup>+/+</sup> and G6PD<sup>+/-</sup> mice: (Q) increased nuclear diameter of brainstem nuclei. (R) Silver staining of cytoplasmic lipofuscin. (S) Thickening and neoplastic proliferation of the brainstem meninges. All sections are  $\times 400$  magnification, unless otherwise noted.

The neuronal population of the striatum and hypothalamus was interpreted to be relatively normal, with no apparent difference between G6PD-normal and G6PD-deficient mice. Histological findings in the cerebellum, cortex, hippocampus and brainstem of homozygous G6PD-deficient females and hemizygous-deficient males were similar to those observed in the heterozygous G6PD-deficient females.

The Purkinje cell total count in the cerebellum for 10 fields was  $55.0 \pm 3.6$  in G6PD<sup>+/+</sup> mice, and  $25.7 \pm 7.6$  in G6PD<sup>+/-</sup> mice, indicating a 53% reduction in G6PD<sup>+/-</sup> mice compared to G6PD<sup>+/+</sup> controls ( $p < 0.001$ ) (Figure 5). No visible ataxia or other motor deficits were apparent.

**Brain G6PD Activity.** Whole brain G6PD activity was decreased respectively to 40.7% and 16.1% of normal in heterozygous and homozygous G6PD-deficient mice compared to G6PD-normal mice (Figure 6). Regional differences in G6PD activity were evident in G6PD-normal mice, with activity varying 3.0-fold increasing from hippocampus, cortex, striatum, olfactory bulb, substantia nigra, brain stem and cerebellum (Figure 7). A similar 2.8-fold regional variation was observed in heterozygous G6PD-deficient mice, increasing from hippo-

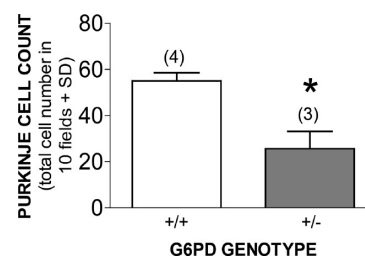


**Figure 5.** Quantitative analysis of Purkinje cells of the cerebellum in aged G6PD-normal and heterozygous G6PD-deficient mice. Purkinje cells were counted in 10 distinct fields at  $40\times$  to give a total of cells for each sample. There was a 54% decrease in cell number in the G6PD-deficient mice compared to G6PD-normal controls (asterisk indicates  $p < 0.0009$ ), consistent with the semiquantitative histological assessment.

campus, striatum, cortex, substantia nigra, olfactory bulb, cerebellum and brain stem. A greater 4.3-fold variation was observed in homozygous G6PD deficient-mice, increasing from hippocampus, striatum, substantia nigra, cortex, brain stem, olfactory bulb and cerebellum.

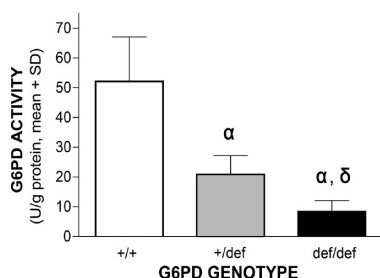


**Figure 6.** G6PD activity in whole brains of aged G6PD-normal and G6PD-deficient mice.  $\alpha$  indicates a decrease from G6PD<sup>+/+</sup> mice ( $p < 0.001$ ), and  $\delta$  indicates a decrease from G6PD<sup>+/def</sup> ( $p < 0.001$ ).  $N = 3, 6,$  and  $4$  respectively for G6PD<sup>+/+</sup>, G6PD<sup>+/def</sup>, and G6PD<sup>def/def</sup> groups.

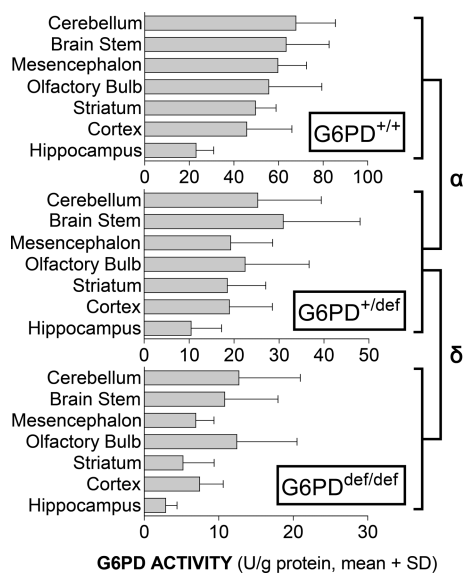


**Figure 7.** G6PD activity in specific brain regions of aged G6PD-normal and G6PD-deficient mice. Note the scale differences in the X axes.  $\alpha$  indicates a difference between G6PD<sup>+/+</sup> and G6PD<sup>+/def</sup> groups, or G6PD<sup>+/def</sup> and G6PD<sup>def/def</sup> groups, in G6PD activity for the same brain region ( $p < 0.001$ ).  $N = 3, 6,$  and  $4$  for G6PD<sup>+/+</sup>, G6PD<sup>+/def</sup>, and G6PD<sup>def/def</sup>.

In comparing regional brain DNA oxidation and G6PD activity in the same mice, in both G6PD-normal and homozygous G6PD-deficient mice, brain regions with the lowest (hippocampus) and highest (cerebellum) G6PD activities showed respectively higher and lower levels of DNA oxidation, suggesting that extremes of G6PD activity may be an important determinant of regional ROS-mediated macromolecular damage (Figure 8). This association was not evident in tissues with intermediary G6PD activities.

In summary, the striatum of G6PD-deficient mice exhibited no increase in oxidative DNA damage or histological changes. Similarly, no significant pathological changes were reported in the hypothalamus as well as in the areas associated with the mesencephalon and diencephalon. In contrast, the cortex, hippocampus and cerebellum exhibited both enhanced DNA oxidation and degenerative histological changes in G6PD-deficient mice. The brainstem, which showed histological changes, exhibited a small but nonsignificant increase in DNA oxidation determined by HPLC, and no increase by immunohistochemistry.

Our studies used both males and females together as we did not find any differences between sexes in our observations.

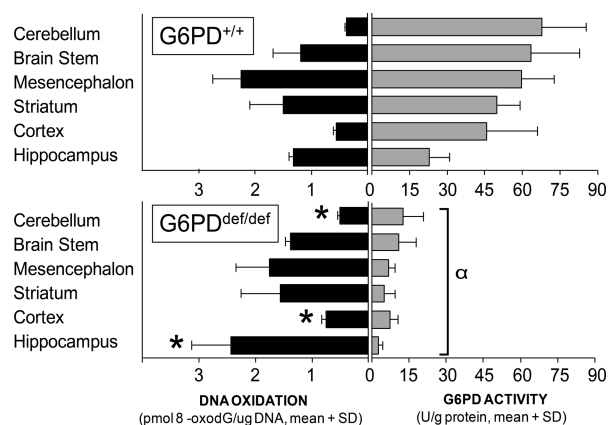


**Figure 8.** Relation of regional DNA oxidation and G6PD activity in G6PD<sup>+/+</sup> and G6PD<sup>def/def</sup> mice. Oxidatively damaged DNA was assessed by 8-oxodG formation using HPLC-EC. G6PD activity was measured by a kinetic assay measuring the formation of NADPH. (DNA oxidation: G6PD<sup>+/+</sup>,  $n = 4$ ; G6PD<sup>def/def</sup>,  $n = 6$ . G6PD activity: G6PD<sup>+/+</sup>,  $n = 3$ ; G6PD<sup>def/def</sup>,  $n = 4$ .) \* indicates an increase in DNA oxidation compared to G6PD-normal mice ( $p < 0.05$ ).  $\alpha$  indicates a decrease in activity from G6PD<sup>+/+</sup> mice for each of the brain regions matched to the same brain region in the G6PD<sup>def/def</sup> mice ( $p < 0.001$ ).

## DISCUSSION

The increased endogenous oxidative DNA damage in regions of the brain associated with enhanced neuropathological damage in aged G6PD-deficient mice suggests that G6PD is important in protecting the brain from ROS-mediated neurodegeneration associated with aging. Remarkably, oxidative damage and neurodegeneration were enhanced in aged heterozygous as well as homozygous G6PD-deficient mice. Given that G6PD activity in this strain is maximally decreased by only about 30% in heterozygous G6PD-deficient mice, depending upon the tissue,<sup>5</sup> the enhanced susceptibility observed with even a heterozygous deficiency indicates that even the modest decrease in G6PD activity associated with the loss of one copy of the gene carries an increased lifetime risk of neurodegeneration. In comparison with other organs, the CNS may for a number of biochemical, physiological and anatomical reasons be especially vulnerable to ROS-mediated injury. Endogenous ROS may be generated from numerous sources, including (1) the relatively high level of CNS oxidative metabolic activity (mitochondrial respiration); (2) high concentrations of non-heme iron and ascorbic acid; (3) glutamate-mediated excitotoxicity and a disruption in Ca<sup>2+</sup> homeostasis; (4) Ah receptor-mediated oxidative stress; (5) auto-oxidation of neurotransmitters; (6) redox cycling of endobiotics and xenobiotics with catechol structures; (7) as well as various neuronal enzyme-catalyzed reactions, including ROS formation via the metabolism of endobiotics and xenobiotics by prostaglandin H synthase in the endoplasmic reticulum (ER) and nuclear membrane, and cytochromes P450 in the ER.<sup>23–27</sup> The lifetime assault of relatively high levels of oxidative stress and accumulation of macromolecular damage, coupled with the relatively low CNS levels of antioxidative enzymes, such as catalase and glutathione peroxidase, compared to the liver or kidney,<sup>28</sup> may render the neural anatomical network vulnerable to disruption. Given the nonreplicating nature of neuronal cells, such ROS-mediated effects cause permanent and cumulative damage to the CNS.



The neurodegenerative mechanism in G6PD-deficient mice could involve increased ROS-dependent signal transduction and/or ROS-initiated oxidative damage to cellular macromolecules, including DNA, RNA, proteins and lipids. We focused on oxidative DNA damage as a potential macromolecular target involved in neurodegeneration since that molecular lesion appears to contribute to the embryopathic mechanism of some ROS-initiating teratogens,<sup>29</sup> including neurodevelopmental deficits,<sup>30</sup> as well contributing to neurodegeneration initiated by amphetamines,<sup>26,27</sup> and by some endogenous neurotransmitters and their precursors and metabolites.<sup>24</sup> DNA oxidation also can be considered as a biomarker for oxidative stress and the concomitant involvement of other potential ROS-dependent mechanisms of toxicity. Analogous to the theory of carcinogenesis,<sup>31</sup> ROS might be involved via macromolecular damage in the initiation of neurodegeneration, and/or via signal transduction in the “promotion/progression” of a degenerative process initiated by other mechanisms.

In the aged G6PD-deficient mice, there was a remarkable association of increased oxidatively damaged DNA (8-oxo-dG, a marker for increased HO<sup>•</sup>), determined by HPLC and/or immunohistochemistry, and neurodegenerative changes in the frontal cortex, hippocampus and cerebellum, as well as a converse absence of oxidative DNA damage and neurodegeneration in the striatum, consistent with a causative role for oxidative stress, and possibly oxidative DNA damage in particular, in the mechanism of neurodegeneration. The one exception to this pattern was the brainstem, wherein increased DNA oxidation was not detected by HPLC or immunohistochemistry, but increased pathological changes were evident in G6PD-deficient mice. The enhanced neurodegenerative effects in this particular brain region may result from a lower level of ROS-dependent signal transduction rather than macromolecular damage, and/or may be codependent upon regionally specific expression of other antioxidative enzymes as discussed below. In addition, we observed a similar decrease on G6PD activity in all brain areas measured but DNA oxidation and morphological changes were only seen in selected brain areas. Pathways regulating the endogenous formation of ROS, levels of antioxidants and other antioxidative enzymes, and levels of enzymes involved in DNA repair all likely differ not only among tissues, but among cell types. If these assumptions are correct, one would expect that the neurodegenerative impact of a G6PD-deficiency would vary among tissues and cell types, as observed in our study. There were no apparent gender differences in the semiquantitative histological observations, although further detailed morphometrics are needed to address this topic and also to definitively quantify the pathological findings observed in different brain sections.

Hereditary G6PD deficiencies, which are the most common human enzymopathies, may accordingly constitute an important risk factor for some neurodegenerative diseases. In addition to the neuroprotective relevance of G6PD itself in the adult brain, the expression of G6PD has been shown to be coordinately modulated with that of other antioxidative enzymes, including glutathione peroxidase and glutathione reductase, in the developing and adult rat brain.<sup>32,33</sup> The mechanism for this coordinated expression is unknown; however, it is thought that nerve growth factor (NGF) and insulin-like growth factor (IGF), which respond to changes in oxidant levels, may act as transcriptional regulators of these genes.<sup>34,35</sup> Hence, in addition to G6PD deficiencies, other

antioxidative defense mechanisms may be compromised, which would increase susceptibility of the brain to ROS-mediated oxidative stress and subsequent neuronal damage.

Our studies showing increased endogenous ROS-mediated oxidative damage and neuronal cell death in specific brain regions and cell types particularly in G6PD-deficient mice are associated with areas of high G6PD expression. Histochemical and immunohistochemical analyses revealed that the highest expression of cerebellar G6PD activity and protein was found in the Purkinje cells<sup>8,36</sup> and later was found to be colocalized with NADPH-dependent enzymes including NADPH-cytochrome P450 reductase and glutathione reductase.<sup>37</sup> We found that the absence of even one copy of the G6PD gene resulted in increased DNA oxidation in Purkinje cells, with a pathological loss of these cells and atrophy of the survivors. This suggests that G6PD expression is required for Purkinje cell viability and possibly for normal functioning of these cells. Previously, we reported the brain activities of G6PD in this strain were approximately 50, 35, and 10 U/g protein in wild-type, heterozygous, and homozygous-deficient mice, respectively,<sup>5</sup> and the current results suggest that activity higher than 35 U/g protein is required at least in mice to protect against ROS-initiated neurodegeneration. G6PD activity may be particularly important in the hippocampus, where increased neuronal G6PD and sulfhydryl levels were found in patients with Alzheimer's disease, presumably in compensation for increased oxidative stress in that region.<sup>14</sup> The levels of CuZnSOD mRNA and protein are particularly high in hippocampal pyramidal neurons and granular cells,<sup>38</sup> which in the absence of adequate G6PD-mediated detoxification may result in H<sub>2</sub>O<sub>2</sub> overproduction and peroxidative damage within these cells. In addition to the cytoprotective role of G6PD against ROS-mediated oxidative damage, G6PD may be required for normal cell growth by providing NADPH for redox regulation.<sup>33,39,40</sup>

The study herein is the first to show enhanced endogenous DNA oxidation in specific brain regions as a consequence of decreased G6PD activity in aged mice, and the associated regionally and cellularly specific neurodegenerative changes. The carcinogenic implications of G6PD deficiency in brain have been investigated in another study employing young mice that contained the X-ray-induced low efficiency allele of G6PD.<sup>41</sup> The brains of these G6PD-deficient males exhibited a decrease in the ratio of reduced glutathione to oxidized glutathione, an accumulation of promutagenic etheno DNA adducts secondary to lipid peroxidation, and an increased somatic mutation rate suggesting an enhanced risk for brain cancer. If such molecular events occur in the strain of aged G6PD-deficient mice used herein, they also could contribute to neurodegeneration. However, no enhanced risk for brain cancer has been reported, and we found no evidence for enhanced carcinogenesis in any tissue of the aged G6PD-deficient mice herein (Loniewska and Wells, unpublished). It may be that the promutagenic etheno DNA adducts in young G6PD-deficient mice observed by Felix and co-workers have less functional consequences than the 8-oxo-dG lesions measured herein in aged G6PD-deficient mice. The 8-oxo-dG lesion has also been implicated in the molecular mechanism of embryopathies and neurodevelopmental deficits caused by ROS-initiating teratogens, likely via nonmutagenic mechanisms involving alterations in gene transcription.<sup>29</sup> A similar mechanism has been implicated in the potential neurodegenerative effects of endogenous<sup>24</sup> and amphetamine-enhanced<sup>26,27</sup> oxidative stress. Further studies of learning and memory, and sensorimotor coordination, will be necessary

to determine the functional consequences of the molecular lesions and neurodegenerative cellular changes observed herein.

When G6PD activity was selectively overexpressed in the dopaminergic nigrostriatal system of mice, it was protective against the toxic effects of the well studied neurotoxin 1-methyl-4-phenyl-1,2,3,6-tetrahydropyridine (MPTP).<sup>42</sup> As with our results, these findings provided evidence that G6PD function has protective potential in the brain. Further gene expression studies in these G6PD-overexpressing mice displayed changes mainly in the expression of proteins related to antioxidant defense, detoxification, and synaptic function.<sup>43</sup>

G6PD deficiency impairs the ability to generate NADPH, which is required for the regeneration of GSH by NADPH-dependent glutathione reductase (Figure 1). The loss of GSH in turn prevents the detoxification of ROS by GSH peroxidases, thus leading to increased ROS levels. However, we cannot rule out a contributing role for catalase in protecting against oxidative stress in the brain. Similar to glutathione reductase, catalase also requires NADPH for normal function, although in this case NADPH binds to catalase and prevents the formation of inactive catalase (compound II), as well as mediating the rapid reduction of catalase compound II back to its active form.<sup>44,45</sup> Impaired catalase activity was found to contribute largely to H<sub>2</sub>O<sub>2</sub>-mediated enhancement of oxidant sensitivity of G6PD-deficient erythrocytes. However, it should be noted that some catalase activity did remain in the G6PD-deficient cells since catalase activity did not drop below 50% of its initial level.<sup>46</sup> Furthermore, the amount of NADPH required for the prevention of catalase inactivation is very low (below 0.1  $\mu$ M) *in vivo*, and the reduction of catalase compound II to the active form (compound I) is known to occur in the absence of NADPH, albeit at much slower rates.<sup>44</sup> Therefore, a contribution from catalase inactivation may be more likely with xenobiotic-enhanced oxidative stress than with endogenous oxidative stress in the face of a G6PD deficiency.

Most individuals with a G6PD deficiency are normally asymptomatic, but can exhibit a clinical syndrome in response to an enhanced oxidative insult or exogenous factors (e.g., xenobiotics, ingestion of fava beans). Although some deficiencies belonging to class I of G6PD variants, which exhibit the most severe deficiency, are associated with chronic nonspherocytic hemolytic anemia,<sup>1</sup> there is no link to date between a specific genetic G6PD variant and a single clinical syndrome. Some of the highest prevalence rates reside in tropical Africa, the Middle East, tropical and subtropical Asia, areas of the Mediterranean and Papua New Guinea, with the incidence of G6PD deficiency approaching 60% in some populations.<sup>47</sup> In such populations, based on the results of our mouse studies, neurodegeneration associated with aging should be considered as a potential outcome in molecular epidemiological studies of G6PD deficiencies, particularly among more severely deficient variants.

## CONCLUSION

In summary, our studies provide the first direct evidence that G6PD deficiency can result in the accumulation of ROS-mediated oxidative damage to DNA in specific areas of the brain with aging. The increased levels of oxidative DNA damage in different brain regions and cell types were associated with pathological changes, including the loss of Purkinje cells, increased neuronal nuclear diameter, increased vacuolation and increased prevalence of chromatolytic neurons. These results suggest a novel role for G6PD in neuroprotection in addition to

its known developmental<sup>5</sup> and hematological<sup>1</sup> importance. In light of the susceptibility of even heterozygous deficient mice observed herein, and the high prevalence of human G6PD deficiencies, this factor may also prove to be an important risk determinant for neurodegenerative diseases.

## METHODS

**Chemicals.** 8-Hydroxy-2'-deoxyguanosine was obtained from Cayman Chemical Co. Nuclease P1 and *Escherichia coli* alkaline phosphatase were obtained from Sigma-Aldrich, chloroform:isoamyl alcohol:phenol (CIP, 24:1:25) and *DdeI* restriction enzyme from Life Technologies, Inc., and proteinase K from Roche Diagnostics. PCR primers were purchased from ACGT Corporation. Taq polymerase and dNTPs were purchased from Perkin-Elmer. All other reagents used were of analytical or HPLC grade.

**Animals.** Female and male mutant G6PD-deficient mice<sup>16</sup> (Medical Research Council, U.K.), 20–30 g, 1.5–2.0 years of age, were housed four per plastic cage with ground corn cob bedding (Beta Chip, Northeastern Products Corp.). The basis of the mutation is an ethylnitrosourea-induced A–T transversion mutation in the exon 1 of the G6PD gene, which is believed to cause a splicing error during post-translational processing. Animals were kept in a temperature-controlled room with a 12 h light/dark cycle automatically maintained. Food (Laboratory Rodent Chow 5001; Ralston Purina) and tap water were provided *ad libitum*. All animals were monitored regularly by a veterinarian and found to be in overtly normal health, with no premature deaths in the colony. All G6PD-deficient genotypes were confirmed as described below. These studies were approved by the University of Toronto Animal Care Committee in accordance with the standards of the Canadian Council on Animal Care.

**Genotyping.** Mouse tail snips were obtained from the mice, and DNA was subsequently isolated from each sample using a standard DNA extraction kit (QIAGEN, Inc.). Purified DNA (100 to 300 ng) was added to a final concentration of 1X PCR buffer, 0.2 mM dNTPs, 1.5 mM MgCl<sub>2</sub>, 0.5  $\mu$ M forward and reverse primers, ddH<sub>2</sub>O and 0.04 unit of Taq polymerase. The G6PD mouse PCR primers (sense, 5'-GGAACTGGCTGTGCGCTAC-3'; antisense, 5'-TCAGCTCCG-GCTCTCTTCTG-3') were made between exon 1 and intron 1, which are designed to generate a 269 bp product targeted around the reported mutation site.<sup>17</sup> The final reaction volume was 30  $\mu$ L. Samples were placed in a thermal cycler (Eppendorf Mastercycler Gradient, Eppendorf Scientific, Inc.) and run under the following conditions: 94 °C, 2 min; 94 °C, 20 s; 58 °C, 20 s; 72 °C, 30 s for 35 cycles and a final extension step of 72 °C, 5 min and kept at 4 °C until ready for digestion. PCR products were digested using *DdeI* restriction enzyme at 37 °C for at least 1 h. Digested PCR samples were combined with 6X gel loading buffer (0.25% bromophenol blue; 0.25% xylene cyanol and 15% Ficoll type 400 in ddH<sub>2</sub>O) and loaded onto a 3% agarose gel containing ethidium bromide. The agarose gel was viewed under UV light and photographed.

Upon *DdeI* digestion, fragments of 214 bp and 55 bp were produced for G6PD<sup>+/+</sup> or G6PD<sup>+/y</sup> mice, no change in the molecular size (269 bp) in G6PD<sup>def/def</sup> or G6PD<sup>def/y</sup> mice, and all three fragments in G6PD<sup>+/def</sup> mice.<sup>5</sup>

**Animal Treatment and Dissection.** The mice were anesthetized by isoflurane and killed by cervical dislocation. For DNA oxidation to be quantified by HPLC, the brains of untreated 1.5 to 2 year old female G6PD-normal and -deficient mice were rinsed with ice-cold 1.15% (w/v) KCl solution and subsequently microdissected on ice to obtain the cortex, hippocampus, striatum, mesencephalon/diencephalons, brainstem and cerebellum, which were immediately snap frozen in liquid nitrogen and stored at –80 °C until the day of the assay.

For H&E staining and immunohistochemistry, the brains of the female and male G6PD-deficient mice were perfused with PBS, followed by 10% neutral buffered formalin, isolated and further fixed overnight in formalin before being embedded in paraffin. Paraffin-embedded brains were sectioned into 5  $\mu$ m thick sections and mounted onto glass microscope slides for further H&E staining or immunohistochemical analysis. H&E stained slides were assessed

semiquantitatively for normal signs of aging and pathological indices of neurodegeneration by a veterinary pathologist, Dr. Colin McKerlie (Toronto Centre for Phenogenomics and the Samuel Lunenfeld Research Institute, Toronto), who was blinded to the genotype of the animals. For quantitative assessment, Purkinje cells of the cerebellum were counted on the H&E-stained slides from 4 G6PD<sup>+/+</sup> mice and 3 G6PD<sup>+/-def</sup> mice. For each slide, the mean number of Purkinje cells was determined from 10 randomly selected fields.

**DNA Extraction and Digestion.** Brain regions dissected from female G6PD-normal or -deficient mice were homogenized in 500  $\mu$ L of DNA digestion buffer (100 mM Tris-HCl, pH 8.0, 5 mM EDTA, pH 8.0, 0.2% (w/v) SDS, 200 mM NaCl) and allowed to digest overnight with proteinase K (50  $\mu$ g mL<sup>-1</sup>) at 55 °C. DNA was extracted as described elsewhere.<sup>18</sup> Isolated DNA (RNA free) was then digested with nuclease P1 (67  $\mu$ g mL<sup>-1</sup>) at 37 °C for 30 min, followed by a 60 min incubation with *Escherichia coli* alkaline phosphatase (0.37 units mL<sup>-1</sup>) at 37 °C. The mixture was syringe tip filtered (0.22  $\mu$ m) and analyzed using a high-performance liquid chromatography (HPLC) with an electrochemical (EC) detector.

**Detection of 8-Oxo-2'-deoxyguanosine (8-Oxo-2'-dG).** Oxidation of 2'-dG to 8-oxo-dG was quantified using an isocratic HPLC (series 200, PerkinElmer Instruments LLC) equipped with a 5  $\mu$ m Exsil 80A-ODS C-18 column (5 cm  $\times$  4.6 mm, Jones Chromatography, Ltd.), an electrochemical detector (Coulchem II), a guard cell (model 5020), an analytical cell (model 5010) (Coulchem, ESA Inc.) and an integrator (PerkinElmer NCI 900 Interface). Samples were filtered (0.22  $\mu$ m), injected into the HPLC-EC system and eluted using a mobile phase consisting of 50 mM KH<sub>2</sub>PO<sub>4</sub> buffer (pH 5.5)–methanol (95:5, v/v) at a flow rate of 0.8 mL min<sup>-1</sup> with a detector oxidation potential of +0.4 V.<sup>19</sup> Chromatographs were analyzed using a commercial chromatography software program (TotalChrom version 6.2.0, PerkinElmer Instruments LLC).

**Immunohistochemistry.** Paraffin-embedded mouse brain sections were deparaffinized in xylene, hydrated in decreasing dilutions of ethanol and rinsed in ddH<sub>2</sub>O. Sections were treated with RNase (100  $\mu$ g mL<sup>-1</sup>) for 1 h at 37 °C followed by blocking of endogenous mouse IgG with MOM Mouse IgG blocking reagent (Vector Laboratories) for 3 h. Tissue sections were then incubated with the N45.1 anti-8-oxo-dG antibody (Wako Chemicals, USA), diluted 1:20 overnight at 4 °C, followed by a 1 h incubation with MOM biotinylated horse anti-mouse IgG secondary antibody. To quench endogenous peroxidase, slides were incubated in 3% (v/v) H<sub>2</sub>O<sub>2</sub> in methanol for 30 min at room temperature. Sections were incubated with Vectastain Elite ABC reagent (Vector Laboratories) for 10 min and subsequently detected by DAB reaction. Slides were counterstained, dehydrated with xylene and mounted.

**Glucose-6-phosphate Dehydrogenase Activity in Individual Brain Areas.** Mice were sacrificed by decapitation, and the brain was removed and rinsed in ice cold 1.15% (w/v) KCl. The brain areas were dissected in the order of olfactory bulb, hippocampus, cortex, striatum, substantia nigra, cerebellum and brain stem, and snap frozen in liquid nitrogen. The samples were stored in a -80 °C freezer until analysis. Each sample was homogenized with a hand homogenizer in 500  $\mu$ L of 50 mM Tris-HCl pH 7.4, and the homogenate was sonicated with a hand sonicator (Fisher Scientific 60 Sonic Dismembrator) for 10 s. The homogenates were centrifuged for 30 min at 15000g in a refrigerated microcentrifuge. The pellet was discarded, and the protein content was determined in the supernatant,<sup>20</sup> as was G6PD activity<sup>21</sup> using a modified protocol.<sup>22</sup> Reaction rates for G6PD were determined by UV spectrophotometry (Beckman model DU 640) at 340 nm at 15 s intervals over 5 min. The final activity of G6PD was determined using the following equation: Net optical density  $\times$  40/6200 =  $\mu$ mol/min/mL of clear homogenate (IU mL<sup>-1</sup>).

**Statistical Analysis.** Statistical significance of differences between paired data was determined by the two-tailed Student's *t* test, while multiple comparisons among groups were analyzed by one-way analysis of variance (ANOVA) followed by a Bonferroni post test using GraphPad InStat 3.05 (GraphPad Software, Inc., GraphPad Software, San Rafael, CA). The level of significance was determined to be at *p* < 0.05.

## AUTHOR INFORMATION

### Corresponding Author

\*Faculty of Pharmacy, University of Toronto, 144 College St., Toronto, Ontario, Canada M5S 3M2. E-mail: pg.wells@utoronto.ca. Tel: 416-978-3221.

### Present Address

<sup>§</sup>Drug Safety Evaluation Projects, Sanofi-Aventis US Inc., Bridgewater, NJ 08807.

### Author Contributions

Winnie Jeng: experimental design, performed the majority of studies, analyzed data, and drafted the core components of the manuscript. Margaret M. Loniewska: performed some studies, analyzed data, and drafted components of the manuscript. Peter G. Wells: conceptual basis and grant support, experimental design, supervisory revisions to data analyses, manuscript and figures.

### Funding

These studies were supported by a grant from the Canadian Institutes of Health Research (CIHR). W.J. was supported by a doctoral award from the CIHR/Rx&D Health Research Foundation, and the Covance doctoral fellowship from the Society of Toxicology.

### Notes

The authors declare no competing financial interest.

## ACKNOWLEDGMENTS

The authors would like to thank Dr. Colin McKerlie of the Toronto Centre for Phenogenomics and the Samuel Lunenfeld Research Institute for his analysis of the H&E slides, and Lily Morikawa for paraffin embedding, sectioning and H&E staining of the G6PD-deficient brain samples. Preliminary reports of this research were presented at the 2000 annual meeting of the Society of Toxicology (U.S.A.) [*Toxicological Sciences* (Supplement: The Toxicologist), 54:178 (No. 838), 2000], and the 2005 annual meeting of the Society of Toxicology of Canada [STC Proceedings, abstract no. 26].

## ABBREVIATIONS

ROS, reactive oxygen species; G6PD, glucose-6-phosphate dehydrogenase; NADPH, nicotinamide adenine dinucleotide phosphate; GSH, glutathione; HPLC-EC, high-performance liquid chromatography with electrochemical detection

## REFERENCES

- (1) Luzzatto, L., Mehta, A., and Vulliamy, T. (2001) Glucose-6-phosphate dehydrogenase (Chapter 179), in *The Metabolic and Molecular Basis of Inherited Disease* (Scriver, C. R., Beaudet, A. L., Sly, W. S., and Valle, D., Eds.) 8th ed., pp 4517–4553, McGraw-Hill, New York.
- (2) Cappellini, M. D., and Fiorelli, G. (2008) Glucose-6-phosphate dehydrogenase deficiency. *Lancet* 371, 64–74.
- (3) Nkhoma, E. T., Poole, C., Vannappagari, V., Hall, S. A., and Beutler, E. (2009) The global prevalence of glucose-6-phosphate dehydrogenase deficiency: a systematic review and meta-analysis. *Blood Cells Mol. Dis.* 42, 267–278.
- (4) Minucci, A., Moradkhani, K., Hwang, M. J., Zuppi, C., Giardina, B., and Capoluongo, E. (2012) Glucose-6-phosphate dehydrogenase (G6PD) mutations database: review of the "old" and update of the new mutations. *Blood Cells Mol. Dis.* 48, 154–165.
- (5) Nicol, C. J., Zielenski, J., Tsui, L. C., and Wells, P. G. (2000) An embryoprotective role for glucose-6-phosphate dehydrogenase in developmental oxidative stress and chemical teratogenesis. *FASEB J.* 14, 111–127.



- (6) Corcoran, C. M., Fraser, P., Martini, G., Luzzatto, L., and Mason, P. J. (1996) High-level regulated expression of the human G6PD gene in transgenic mice. *Gene* 173, 241–246.
- (7) Kletzien, R. F., Harris, P. K., and Foellmi, L. A. (1994) Glucose-6-phosphate dehydrogenase: a “housekeeping” enzyme subject to tissue-specific regulation by hormones, nutrients, and oxidant stress. *FASEB J.* 8, 174–181.
- (8) Biagiotti, E., Guidi, L., Capellacci, S., Ambrogini, P., Papa, S., Del Grande, P., and Ninfali, P. (2001) Glucose-6-phosphate dehydrogenase supports the functioning of the synapses in rat cerebellar cortex. *Brain Res.* 911, 152–157.
- (9) Cammer, W., and Zimmerman, T. R., Jr. (1982) Glycerolphosphate dehydrogenase, glucose-6-phosphate dehydrogenase, lactate dehydrogenase and carbonic anhydrase activities in oligodendrocytes and myelin: comparisons between species and CNS regions. *Brain Res.* 282, 21–26.
- (10) Philbert, M. A., Beiswanger, C. M., Roscoe, T. L., Waters, D. K., and Lowndes, H. E. (1991) Enhanced resolution of histochemical distribution of glucose-6-phosphate dehydrogenase activity in rat neural tissue by use of a semipermeable membrane. *J. Histochem. Cytochem.* 39, 937–943.
- (11) Ho, H. Y., Cheng, M. L., Lu, F. J., Chou, Y. H., Stern, A., Liang, C. M., and Chiu, D. T. (2000) Enhanced oxidative stress and accelerated cellular senescence in glucose-6-phosphate dehydrogenase (G6PD)-deficient human fibroblasts. *Free Radical Biol. Med.* 29, 156–169.
- (12) Preville, X., Salvemini, F., Giraud, S., Chaufour, S., Paul, C., Stepien, G., Ursini, M. V., and Arrigo, A. P. (1999) Mammalian small stress proteins protect against oxidative stress through their ability to increase glucose-6-phosphate dehydrogenase activity and by maintaining optimal cellular detoxifying machinery. *Exp. Cell Res.* 247, 61–78.
- (13) Palmer, A. M. (1999) The activity of the pentose phosphate pathway is increased in response to oxidative stress in Alzheimer's disease. *J. Neural Transm.* 106, 317–328.
- (14) Russell, R. L., Siedlak, S. L., Raina, A. K., Bautista, J. M., Smith, M. A., and Perry, G. (1999) Increased neuronal glucose-6-phosphate dehydrogenase and sulfhydryl levels indicate reductive compensation to oxidative stress in Alzheimer disease. *Arch. Biochem. Biophys.* 370, 236–239.
- (15) Longo, L., Vanegas, O. C., Patel, M., Rosti, V., Li, H., Waka, J., Merghoub, T., Pandolfi, P. P., Notaro, R., Manova, K., and Luzzatto, L. (2002) Maternally transmitted severe glucose 6-phosphate dehydrogenase deficiency is an embryonic lethal. *EMBO J.* 21, 4229–4239.
- (16) Pretsche, W., Charles, D. J., and Merkle, S. (1988) X-linked glucose-6-phosphate dehydrogenase deficiency in *Mus musculus*. *Biochem. Genet.* 26, 89–103.
- (17) Sanders, S., Smith, D. P., Thomas, G. A., and Williams, E. D. (1997) A glucose-6-phosphate dehydrogenase (G6PD) splice site consensus sequence mutation associated with G6PD enzyme deficiency. *Mutat. Res.* 374, 79–87.
- (18) Liu, L., and Wells, P. G. (1995) DNA oxidation as a potential molecular mechanism mediating drug-induced birth defects: phenytoin and structurally related teratogens initiate the formation of 8-hydroxy-2'-deoxyguanosine in vitro and in vivo in murine maternal hepatic and embryonic tissues. *Free Radical Biol. Med.* 19, 639–648.
- (19) Winn, L. M., and Wells, P. G. (1997) Evidence for embryonic prostaglandin H synthase-catalyzed bioactivation and reactive oxygen species-mediated oxidation of cellular macromolecules in phenytoin and benzo[a]pyrene teratogenesis. *Free Radical Biol. Med.* 22, 607–621.
- (20) Bradford, M. M. (1976) A rapid and sensitive method for the quantitation of microgram quantities of protein utilizing the principle of protein-dye binding. *Anal. Chem.* 72, 248–254.
- (21) Glock, G. E., and McLean, P. (1953) Further studies on the properties and assay of glucose 6-phosphate dehydrogenase and 6-phosphogluconate dehydrogenase of rat liver. *Biochem. J.* 55, 400–408.
- (22) Ninfali, P., Aluigi, G., and Pompella, A. (1997) Methods for studying the glucose-6-phosphate dehydrogenase activity in brain areas. *Brain Res. Protoc.* 1 (4), 357–363.
- (23) Coyle, J. T., and Puttfarcken, P. (1993) Oxidative stress, glutamate, and neurodegenerative disorders. *Science* 262, 689–695.
- (24) Goncalves, L. L., Ramkissoon, A., and Wells, P. G. (2009) Prostaglandin H synthase-1-catalyzed bioactivation of neurotransmitters, their precursors and metabolites: oxidative DNA damage and electron spin resonance spectroscopy studies. *Chem. Res. Toxicol.* 22, 842–852.
- (25) Hassoun, E. A., Wilt, S. C., Devito, M. J., Van Birgelen, A., Alsharif, N. Z., Birnbaum, L. S., and Stohs, S. J. (1998) Induction of oxidative stress in brain tissues of mice after subchronic exposure to 2,3,7,8-tetrachlorodibenzo-p-dioxin. *Toxicol. Sci.* 42, 23–27.
- (26) Jeng, W., Ramkissoon, A., Parman, T., and Wells, P. G. (2006) Prostaglandin H synthase-catalyzed bioactivation of amphetamines to free radical intermediates that cause CNS regional DNA oxidation and nerve terminal neurodegeneration. *FASEB J.* 20, 638–650.
- (27) Jeng, W., and Wells, P. G. (2010) Reduced 3,4-methylenedioxymethamphetamine (Ecstasy)-initiated oxidative DNA damage and neurodegeneration in prostaglandin H synthase-1 knockout mice. *ACS Chem. Neurosci.* 1 (5), 366–380.
- (28) Sohal, R. S., Sohal, B. H., and Brunk, U. T. (1990) Relationship between antioxidant defenses and longevity in different mammalian species. *Mech. Ageing Dev.* 53, 217–227.
- (29) Wells, P. G., McCallum, G. P., Chen, C. S., Henderson, J. T., Lee, C. J. J., Perstin, J., Preston, T. J., Wiley, M. J., and Wong, A. W. (2009) Oxidative stress in developmental origins of disease: teratogenesis, neurodevelopmental deficits and cancer. *Toxicol. Sci.* 108, 4–18.
- (30) Wong, A. W., McCallum, G. P., Jeng, W., and Wells, P. G. (2008) Oxoguanine glycosylase 1 (OGG1) protects against methamphetamine-enhanced fetal brain oxidative DNA damage and neurodevelopmental deficits. *J. Neurosci.* 28, 9047–9054.
- (31) Klaunig, J. E., and Kamendulis, L. M. (2007) Chemical carcinogenesis (Chapter 8), in *Toxicology: The Basic Science of Poisons* (Klaassen, C. D., Ed.) 7th ed., pp 329–379, McGraw-Hill, New York.
- (32) Ninfali, P., Aluigi, G., and Pompella, A. (1998) Postnatal expression of glucose-6-phosphate dehydrogenase in different brain areas. *Neurochem. Res.* 23, 1197–1204.
- (33) Ninfali, P., Cuppini, C., and Marinoni, S. (1996) Glucose-6-phosphate dehydrogenase and glutathione reductase support antioxidant enzymes in nerves and muscles of rats during nerve regeneration. *Restor. Neurol. Neurosci.* 10, 69–75.
- (34) Harris, E. D. (1992) Regulation of antioxidant enzymes. *J. Nutr.* 122, 625–626.
- (35) Yu, B. P. (1994) Cellular defenses against damage from reactive oxygen species. *Physiol. Rev.* 74, 139–162.
- (36) Biagiotti, E., Guidi, L., Del Grande, P., and Ninfali, P. (2003) Glucose-6-phosphate dehydrogenase expression associated with NADPH-dependent reactions in cerebellar neurons. *Cerebellum* 2, 178–183.
- (37) Ferri, P., Biagiotti, E., Ambrogini, P., Santi, S., Del Grande, P., and Ninfali, P. (2005) NADPH-consuming enzymes correlate with glucose-6-phosphate dehydrogenase in Purkinje cells: an immunohistochemical and enzyme histochemical study of the rat cerebellar cortex. *Neurosci. Res.* 51, 185–197.
- (38) Ceballos-Picot, I., Nicole, A., and Sinet, P. M. (1992) Cellular clones and transgenic mice overexpressing copper-zinc superoxide dismutase: models for the study of free radical metabolism and aging. *EXS* 62, 89–98.
- (39) Pandolfi, P. P., Sonati, F., Rivi, R., Mason, P., Grosveld, F., and Luzzatto, L. (1995) Targeted disruption of the housekeeping gene encoding glucose 6-phosphate dehydrogenase (G6PD): G6PD is dispensable for pentose synthesis but essential for defense against oxidative stress. *EMBO J.* 14, 5209–5215.
- (40) Tian, W. N., Braunstein, L. D., Pang, J., Stuhlmeier, K. M., Xi, Q. C., Tian, X., and Stanton, R. C. (1998) Importance of glucose-6-phosphate dehydrogenase activity for cell growth. *J. Biol. Chem.* 273, 10609–10617.
- (41) Felix, K., Rockwood, L. D., Pretsch, W., Nair, J., Bartsch, H., Bornkamm, G. W., and Janz, S. (2002) Moderate G6PD deficiency

increases mutation rates in the brain of mice. *Free Radical Biol. Med.* 32, 663–673.

(42) Mejias, R., Villadiego, J., Pintado, C. O., Vime, P. J., Gao, L., Toledo-Aral, J. J., Echevarria, M., and Lopez-Barneo, J. (2006) Neuroprotection by transgenic expression of glucose-6-phosphate dehydrogenase in dopaminergic nigrostriatal neurons of mice. *J. Neurosci.* 26, 4500–4508.

(43) Romero-Ruiz, A., Mejias, R., Diaz-Martin, J., Lopez-Barneo, J., and Gao, L. (2010) Mesencephalic and striatal protein profiles in mice over-expressing glucose-6-phosphate dehydrogenase in dopaminergic neurons. *J. Proteomics* 73, 1747–1757.

(44) Kirkman, H. N., Galiano, S., and Gaetani, G. F. (1987) The function of catalase-bound NADPH. *J. Biol. Chem.* 262, 660–666.

(45) Kirkman, H. N., Rolfo, M., Ferraris, A. M., and Gaetani, G. F. (1999) Mechanisms of protection of catalase by NADPH. Kinetics and stoichiometry. *J. Biol. Chem.* 274, 13908–13914.

(46) Scott, M. D., Wagner, T. C., and Chiu, D. T. (1993) Decreased catalase activity is the underlying mechanism of oxidant susceptibility in glucose-6-phosphate dehydrogenase-deficient erythrocytes. *Biochim. Biophys. Acta* 1181, 163–168.

(47) Sodeinde, O. (1992) Glucose-6-phosphate dehydrogenase deficiency. *Baillieres Clin. Haematol.* 5, 367–382.